Method of Formation of an Artificial Multiphase Field of a Specified Structure During Phase-Metric Technological Control

D. Surzhik[1], G. Vasilyev[2(✉)], and O. Kuzichkin[2]

[1] Vladimir State University, 23, st. Orlovskaya, Vladimir 602264, Russia
[2] Belgorod National Research University, 85, st. Pobedy, Belgorod 308015, Russia
vasilievgleb@yandex.ru

Abstract. Phasometric control methods in relation to the tasks of technological monitoring of various objects involve the isolation, analysis and tracking of the dynamics of the phases of their transfer functions in real time. At the same time, the number of spatially spaced point sources of the field should correspond to the detail of the network of phasometric control points. In this case, the generated signals can generally be arbitrary, and the differences between their parameters consist in setting certain amplitude-phase ratios that depend on the relative spatial location of the phase control points and point sources. Based on the proposed method, a multiphase field simulation was carried out using the example of geoelectric control, which has shown the effectiveness of phase-measuring methods and devices for recording variations of the object of control with sufficient sensitivity of the measuring installation.

Keywords: Phasometric method · Agular measurements · Multiphase field · Probing signals · Geoelectrics

1 Introduction

The known methods and devices of phase monitoring [1–3] are based on continuous measurements of instantaneous values of phase shift angles between oscillations of physical fields of equal frequency and determination of their parameters and characteristics.

For a pair of signals of the same circular frequency ω, the phase shift $\Delta\varphi$ can be determined through a time delay (time shift) as:

$$\Delta_\varphi = \omega\Delta t = 2\pi f\,\Delta_t = \frac{2\pi f\,\Delta_t}{T} = \frac{360^\circ\Delta t}{T}$$

where T is the period of signals.

According to the provisions of measurement theory, the problem of determining the phase difference of a pair of oscillations $\Delta\varphi$ can be solved in various ways [4–10], allowing their implementation, both in analog and digital form. At the same time, the main classification of methods assumes their differentiation by the type of signals being

A. A. Radionov and V. R. Gasiyarov (Eds.): RusAutoCon 2023, LNEE 1130, pp. 156–165, 2024.
https://doi.org/10.1007/978-3-031-51127-1_15

compared, dividing them into methods for comparing phases of quasi-harmonic and pulse signals, and the second group of methods is less preferable for practical implementation. This is due to the appearance of additional measurement errors in the presence of high-frequency noise; useful or parasitic amplitude modulation of the compared signals; displacement of their zero level; as well as caused by loss of information due to the processes of converting quasi-harmonic signals into pulsed ones.

In the known modifications of the phasometric control method in relation to monitoring tasks [11–13], it is assumed to isolate, analyze and monitor the dynamics of the phase $\Delta\varphi(j\omega, x, y, z)$ of the transfer function of the control object in real time (x, y, z are spatial coordinates). At the same time, the features of various approaches are specific algorithms and methods for generating probing signals to create the necessary multiphase structure of a particular physical field, receiving and primary conversion of measuring signals, as well as processing and interpreting the information contained in them.

2 Method of Formation of a Multiphase Field of a Given Structure

The use of the thermoelectric method of obtaining heat and cold makes it possible to implement on its basis a climate control system for agro-industrial facilities [12, 13]. The microclimate control with its help is carried out under the action of control variables in the form of control currents I_C, which are functionals of the desired temperature values of the T_D and the results of temperature measurements using sensors T_S.

In order for a certain phase value of one or another excited physical field to be created at each point of the control object, it is necessary and sufficient that the minimum number of point radiating poles-field sources is equal to two ($I \geq 2$). In addition, these point sources that excite an artificial multiphase field must be spatially spaced, and supplied to them probing signals are time–varying. In this case, the shape of the signals can generally be arbitrary, and the differences between their parameters consist in setting certain amplitude-phase ratios [11–13], depending on the relative spatial location of the control object and point sources. Such an approach to signal generation can be analytically written as

$$s_i(t, x_i, y_i, z_i) = s(t, x_i, y_i, z_i, A_i, \varphi_{0i}) \tag{1}$$

where $i = 1....I$, I is the number of point radiating source poles, A_i - the amplitude of the i-th probing signal, φ_{0i} - the initial phase of the i-th probing signal.

Thus, devices for generating probing signals based on phasometric control methods should be able to control not only the frequency, but also the amplitude and phase of synthesized signals, and to ensure increased accuracy, sensitivity and noise immunity of measurements, stability of parameters and phase synchronization for the entire range of operating frequencies of probing.

In accordance with the proposed provisions of the method of forming a multiphase field of a given structure, one of the probing signals with eigenvalues of amplitude and phase is taken as a reference, and the amplitude-phase relations for the remaining signals are set relative to this signal. With this approach, it is convenient to represent

the relationship between signals in an exponential form using complex numbers. In this case, expression (1) will take the following form

$$s_i(t, x_i, y_i, z_i) = A_i(t, x_i, y_i, z_i)e^{j\varphi_{0i}(j\omega, x_i, y_i, z_i)} \tag{2}$$

Thus the set of vectors distributed on the complex plane and constructed in accordance with (2) will reflect the relationship between the amplitude-phase ratios of the probing signals. An example of such a distribution for clarity is shown in Fig. 1, where the case of using four signals as probing is considered, and the signal $s_1(t, x_1, y_1, z_1)$ is taken as a reference and depicted along the real axis for which $\varphi_{01}(t, x_1, y_1, z_1) = 0$.

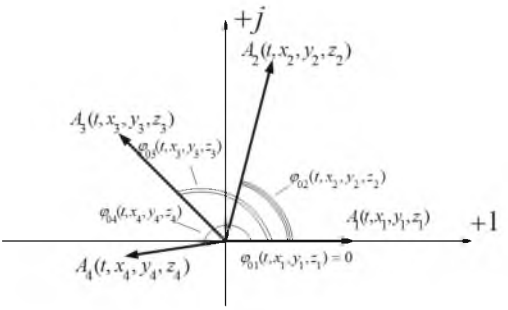

Fig. 1. Vector diagram of the distribution of signals on the complex plane, illustrating the relationship between the amplitude-phase relations of their parameters.

Depending on the characteristics of the controlled object [14–20] and the types of observed processes, the number of point sources can be changed, as well as the parameters of the generating signals coming to them (frequency, amplitude and/or initial phase), which allows the use of phasometric methods and monitoring devices to monitor a variety of processes under different measurement conditions.

3 Modeling of an Artificial Multiphase Low-Frequency Geoelectric Field

We will model a multiphase field using the example of geoelectric control [14, 15]. At the same time, we assume that the complex vector of the geoelectric field strength of the object of control with a resistivity ρ is created by two point radiating poles-sources of complex current $\dot{I} = Ie^{j\varphi}$ and is defined as

$$\vec{E} = \frac{\dot{I}\rho}{2\pi r^2}\frac{\vec{r}}{r} \tag{3}$$

where r and $\vec{r}$ are the distance and radius are the vector from the point radiating pole of the field source to the point pole of the receiver.

The modulus of the geoelectric field strength vector $\vec{\dot{E}} = \vec{\dot{E}}_x + \vec{\dot{E}}_y$ is determined by adding up separately the real and imaginary parts of the projections of the field vector on the coordinate axes x and y (excluding the z axis directed down into the medium):

$$\dot{E} = \sqrt{\mathrm{Re}(\dot{E}_x)^2 + \mathrm{Re}(\dot{E}_y)^2} + j\sqrt{Im(\dot{E}_x)^2 + Im(\dot{E}_y)^2} \tag{4}$$

The phase component of this vector is defined as the arctangent of the ratio of the imaginary and real components:

$$\varphi(\dot{E}) = atan\left(\frac{Im(\dot{E})^2}{\mathrm{Re}(\dot{E})^2}\right) \tag{5}$$

A diagram of a geoelectric installation for modeling is shown in Fig. 2, where *GND* is a point grounding pole.

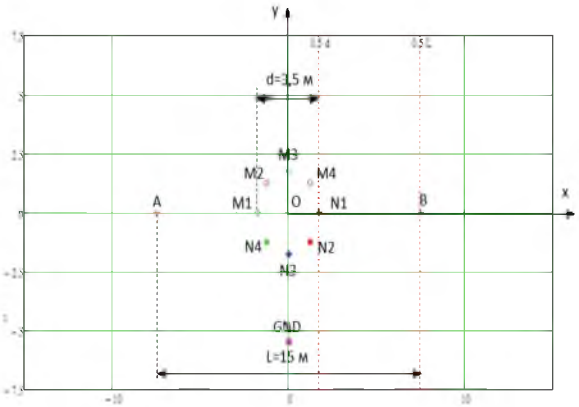

Fig. 2. Diagram of a geoelectric installation for modeling.

In this case, the phase shift between the currents arriving at the point radiating poles-sources A and B is 90°, $L = 15$ m, $d = 3.5$ m, eight point poles-receivers M_i and N_i forming four differential pairs M_iN_i are used to register phase parameters and field characteristics. The amplitudes of the currents of the point radiating poles-sources and the resistivity of the object of control affect only the amplitude component of the generated multiphase electric field, therefore, normalized values are set for them.

Then the electric field strength in accordance with (3) for a given geoelectric installation is defined as

$$\begin{aligned} E(rm) = &\frac{I_1(A - rm)}{2\pi(|A - rm|)^2|A - rm|} + \frac{I_2(B - rm)}{2\pi(|B - rm|)^2|B - rm|} \\ &- \frac{(I_1 + I_2)(GND - rm)}{2\pi(|GND - rm|)^2|GND - rm|} \end{aligned} \tag{6}$$

The first term (6) is the contribution of the electric field caused by the point radiating pole–source A at the point with the radius vector rm, the second term is the contribution

of the point radiating pole-source B, the third term is the contribution of the point pole–grounding GND. The distances from each point radiating source pole to the rm receiving points are defined as vector modules.

The distribution of the phase of the electric field along the x and y coordinates, represented in degrees and obtained on the basis of expressions (4) and (5) taking into account the multiplier $180/\pi$, is shown in Fig. 3 relative to the point radiating pole-source A.

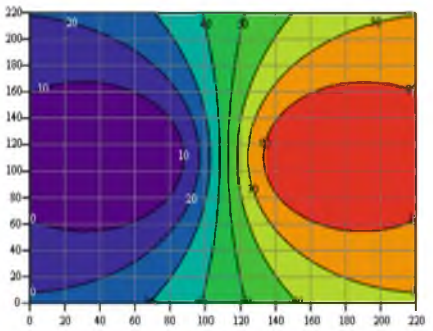

Fig. 3. The result of modeling the phase distribution of the electric field.

Figure 4 shows a family of curves demonstrating changes in the recorded phase of the electric field when the point pole-receiver moves along the coordinate axes (x, y) relative to the point radiating pole-source A, and the step along the ordinate axis takes discrete values $y = 0, 2, 5, 10$ m.

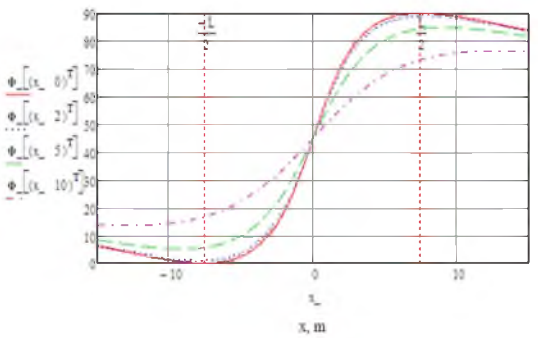

Fig. 4. Graphs of the change in the recorded phase of the electric field when the point pole-receiver moves along the coordinate axes (x, y) relative to the point radiating pole-source A.

The red curve in Fig. 4 (at $y = 0$ m) corresponds to the movement of the point receiver pole along the line AB and gives the largest phase variation from 0° to 90°. When a point receiver pole is shifted vertically up or down by an equal distance, the phase of the field at the receiving point changes in the same way. Figure 5 shows a similar family of curves

showing changes in the recorded phase of the electric field when the point pole-receiver moves away from the center of the setup along the x coordinate. Since the graphs are symmetrical about the origin, the figure shows only their right side for positive values of the x coordinate.

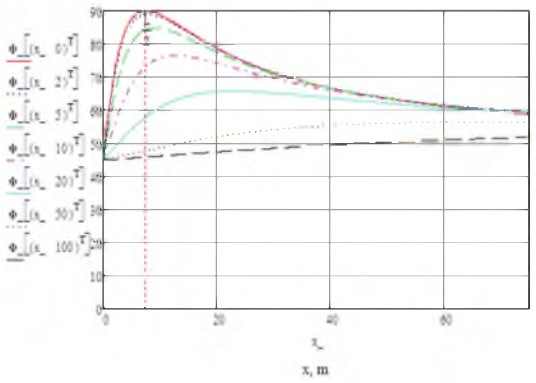

Fig. 5. Graphs of the change in the recorded phase of the electric field when the point pole-receiver moves away from the center of the setup along the x coordinate

It can be seen from the figure that even when the point pole-receiver is removed at a distance of 100 m vertically (black curve, long dotted line), the phase variations with a change in the x coordinate are about 7° (and 14°, taking into account negative x values).

The calculation of the modulus makes it possible, in addition to the analysis of phase characteristics, to construct the distribution of the electric field amplitude in the near-surface part of a homogeneous geological medium.

In the Fig. 6, the distance along the coordinate axes is also taken in decimeters, the amplitude of the electric field is expressed in dB relative to 1 V/m, taking into account the introduced normalizations. Let's consider a similar example for a different scale of a geoelectric installation. In this case, we assume that the phase shift between the currents supplied to the point source poles A and B is also 90°, $L = 110$ cm, $d = 60$ cm.

The distribution of the phase of the electric field in the near-surface part of a homogeneous geological environment for this case is shown in Fig. 7. The dimensions of the axes in this and subsequent figures are centimeters.

Let us complicate the task by considering the case of introducing heterogeneity in a controlled area of the near-surface part of the geological environment. The distribution of the phase of the electric field under these conditions is shown in Fig. 8, and the changes in the phase component of the field are shown in Fig. 9.

As the inhomogeneity, in this case, an additional point pole-grounding is introduced, located to the left of the center of the geoelectric installation (in the direction of the point radiating pole-source A) with the spatial position $x_{GND} = -75$ cm and $y_{GND} = -20$ cm. The current of the point ground pole is taken equal to $-K_{GND}(\dot{I}_A + \dot{I}_B)$, where K_{GND} is the coefficient of current attenuation of the point pole-grounding in the near-surface part of the geological environment ($K_{GND} = 0.03$).

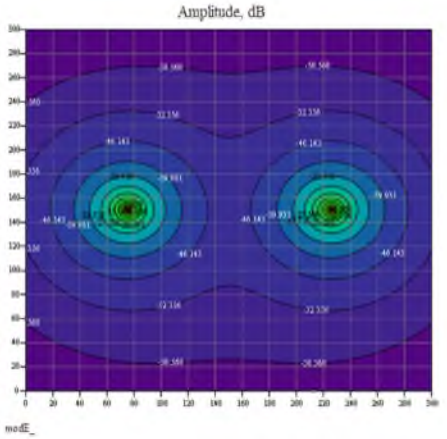

Fig. 6. Distribution of the electric field amplitude in the near-surface part of a homogeneous geological environment.

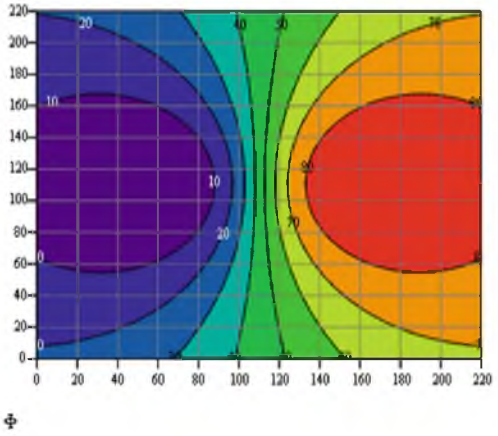

Fig. 7. Distribution of the phase of the electric field in the near-surface part of a homogeneous geological environment.

In Fig. 9, the equiphase contours correspond to the logarithm of the phase deviation from 1 (phase shift 10°) to –4 (phase shift 0.0001°). Figure 9 shows that phase changes of more than 0.1° (contour line 1) are observed in most of the modeling area, which makes it possible to effectively use phase metric methods to register geodynamic processes in the near-surface part of the geological environment with sufficient sensitivity of the measuring setup.

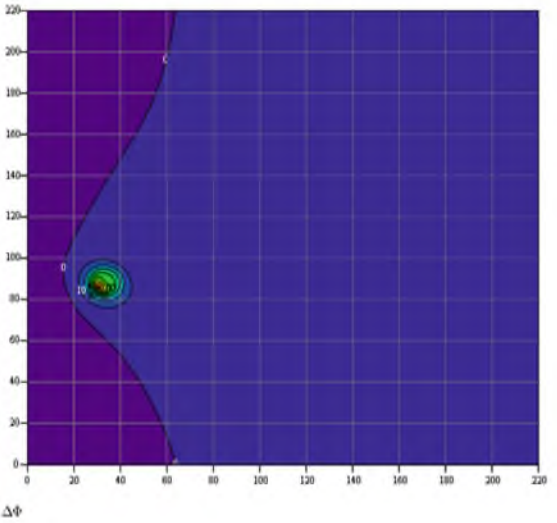

Fig. 8. Distribution of the phase of the electric field in an inhomogeneous geological environment.

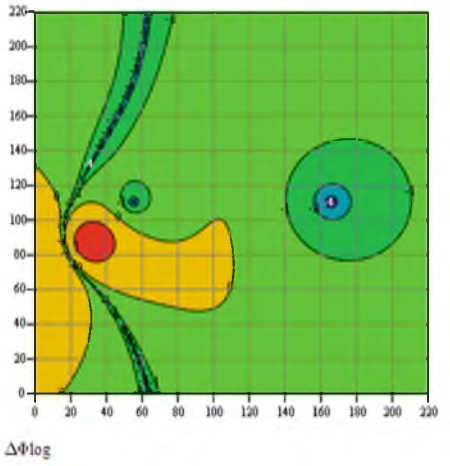

Fig. 9. Changes in the phase component of the electric field in an inhomogeneous geological environment.

4 Conclusion

When using the proposed approach, the object of control is an "equifase surface" (by analogy with an equipotential surface), illustrating the phase distribution of a particular physical field by a set of "equifase isolines" created by each point radiating source pole.

In the Fig. 1, the equifase isolines of the multiphase electric field are constructed in increments of 10, the distance along the coordinate axes is expressed in decimeters. The simulation results determined that the phase point on the poles of the receivers relative to the phase of the radiating point of the pole source of the And take the following

values: $\varphi_{M1} = 21.11°$, $\varphi_{M2} = 27.586°$, $\varphi_{M3} = 45°$, $\varphi_{M4} = 62.414°$, $\varphi_{N1} = 68{,}89°$, $\varphi_{N2} = 62.368°$, $\varphi_{N3} = 45°$, $\varphi_{N4} = 27.632°$.

At the same time, the modification of the modeling problem, due to the artificial introduction of heterogeneity of the control object, does not cause any special difficulties and is solved, for example, by introducing an additional point pole-grounding. The simulation performed under these conditions shows that phase changes of more than 0.1° are observed in most of the modeling area, which makes it possible to effectively use phasometric methods to register variations of the control object with sufficient sensitivity of the measuring installation.

Acknowledgments. The work was carried out with the support of the RSF grant 23-29-10126 "Intelligent system for monitoring the integrity of the railway roadbed". The theory was prepared within the framework of the state task of the Russian Federation "Research and development of complex energy-saving and thermoelectric regenerative systems" application number 2019-1497, subject number FZWG-2020-0034.

References

1. Sergeev, A.G., Krokhin, V.V.: Metrology. Moscow (2001)
2. Novikov, G.A.: Fundamentals of Metrology: Textbook. Ulyanovsk (2010)
3. Sinitsyn, N.F.: Phase Digital Angle Converters, p. 136. Mechanical Engineering, Moscow (1984)
4. Voronov, A.S.: Measurement of the Phase Difference of Signals. Horizons of Education (2007)
5. Ignatiev, V.K., Nikitin, A.V., Orlov, A.A.: Measurement of the phase difference of quasi-harmonic signals in real time. Sci. Educ.: Sci. Ed. Mosc. State Tech. Univ. Named After N.E. **7**, 241–257 (2013)
6. Stepanov, V.V., Matveev, S.A.: Methods of Computer Signal Processing of Radio Communication Systems, pp. 48–54. SOLON-Press, Moscow (2003)
7. Tokmachev, D.A., Poletaev, A.C., Bezrukin, A.G., Chenskiy, A.G.: Synchronization system of an ultra-long-wave interferometer. Instrum. Tech. Exp. **5**, 77–84 (2014). https://doi.org/10.7868/S0032816214050139
8. Transition, N.G.: Measurement of Phase Parameters of Random Signals. Tomsk (1991)
9. Poletaev, A.S., Chenskiy, A.G., Tokmachev, D.A.: Registration of variations of amplitude and phase signals of navigation shift transmitters. In: Interaction of fields and radiation with matter. In: Proceedings of the XIV Conference of Young Scientists. Irkutsk, September 14–18, pp. 252–255 (2015)
10. Poletaev, A.S., Chenskiy, A.G., Grigoriev, K.A.: Monitoring of the lower ionosphere by the method of oblique sounding with SDV radio signals. Bulletin of IrSTU **10**(69), 203–211 (2012)
11. Kuzichkin, O.R., Surzhik, D.I., Vasilyev, G.S., Baknin, M.D.: The phase-metric method of isolating the information component in the distributed processing of geoelectric signals in geoecological monitoring systems. J. Adv. Res. Dyn. Control. Syst. **12**(6), 463–471 (2020)
12. Dorofeev, N.V., Grecheneva, A.V., Kuzichkin, O.R., Surzhik, D.I.: The method of the phase control of the electrical installation during geodynamic monitoring. In: 2018 2nd International Conference on Functional Materials and Chemical Engineering (ICFMCE 2018), MatecWeb of Conferences, vol. 01045, no. 272, pp. 1–13 (2019)

13. Kuzichkin, O.R., Vasilyev, G.S., Grecheneva, A.V., Mikhaleva, E.V.: Application of phase-metric compensation method for geoelectric control of near-surface geodynamic processes. Bull. Electr. Eng. Inform. **9**(3), 898–905 (2020)
14. Khmelevsky, V.K.: Electrical Exploration by the Method of Resistances: Textbook, p. 160. Publishing House of Moscow State University, Moscow (1994)
15. Zhdanov, M.S.: Electrical Exploration: Textbook for Universities. Nedra, Moscow (1986)
16. Korolev, V.A.: Monitoring of the Geological Environment. Publisher MGU, Moscow (1995)
17. Pozdnyakov, A.I., Gulalyev, C.G.: Electrophysical Properties of Some Soils, p. 240. Moscow (2004)
18. Khmelevskoy, V.K., Gorbachev, Y.I., Kalinin, A.V., Popov, M.G.: Geophysics Research Methods: Textbook, p. 232. Stipend. Petropavlovsk-Kamchatsky (2004)
19. Khmelevskaya, V.K., Kostitsyn, V.I.: Fundamentals of Geophysical Methods: Textbook for Universities, p. 400. UN-t, Perm (2010)
20. Khmelevsky, V.C., Bondarenko, V.M.: Electrical Exploration: Handbook of Geophysics in Two Books. Nedra, Moscow (1989)